Rapidly Solidified Fe–Mn–based Shape Memory Alloys

P. Donner, E. Hornbogen, Institut für Werkstoffe, Ruhr–Universität Bochum, D – 4630 Bochum

Introduction

Meltspinning is a method well suited to obtain thin ribbons directly from the melt. This may become of importance for the manufacturing of shape memory alloys, since conventional melting and subsequent plastic deformation of these alloys requires an extensive effort. A further advantage is the formation of homogeneous microstructures without further heat–treatment.
Dendritic growth, associated with local differences in the chemical composition, disappears by rapid solidification from the liquid. High rates of cooling support massiv crystallization, which leads to homogeneous distribution of solution. In addition a favourable microstructure with columnar grains and solidification texture can be achieved by meltspinning; as shown in earlier experiments with NiTi–and copper–based shape memory alloys (1).
Besides these well known shape memory alloys, iron–based alloys have attracted recent attention. Since experiments with Fe–Mn–based alloys have indicated that the shape of thin sheets or wires is of advantage for some applications (2,3), meltspinning offers a favourable method of manufacture.
In this paper, the microstructures resulting from meltspinning and their influence on the martensitic transformation behaviour are reported. Moreover, investigations on the mechanical and shape memory properties are presented. The study was predominantly done on ternary Fe–Mn–Si–specimen, the most promising Fe–Mn–base shape memory alloy. Further on a small amount of silicon was substituted by phosphorous in an Fe–30Mn–5Si alloy to improve the strength of these materials by the mechanism of solid solution hardening.

Materials and Procedures

The compositions of the alloys used for this investigation are given in table 1. The alloys were produced by arc–melting in an Ar–atmosphere. Amounts of 7–10 g were used for meltspinning with quarz nozzles of 1.0–1.5 mm diameter. The ribbons were spun on a 200 mm copper–wheel in a helium atmosphere. Their thickness and, in turn, the cooling–rate was influenced by the circumferential velocities of the wheel (2–50 m/s), the ejection pressures (argon gas at 0.1–1.5 bar) and the angle between nozzle and wheel.
The microstructures were observed by light microscopy, SEM and TEM. The transformation temperatures were measured by differential scanning calorimetry (DSC) with a DuPont Thermal Analyzer 9900. The amount of residual austenite in the martensitic state was determined by X–Ray diffractometry (Mo–K_α).
Tensile test specimens were produced by spark erosion, cutting a special kind of shape from the ribbon (see Fig. 5). The ribbon thickness was determined by SEM and micrometrically The strain was measured with an extensometer clipped between the specimen grips.
The amount of reversible strain and the change of transformation temperatures under stress were measured by applying tensile load parallel to the ribbon–axis. The specimen was positioned in an induction furnace with integrated cooling–pipes (compressed air cooled by N_2) to render possible thermal cycling in a temperature range from –150 °C up to 350 °C.

Alloy	Nominal Composition	EDAX			
		Fe	Mn	Si [wt.%]	P
A	Fe–24Mn–3Si	71.4	24.2	4.4	
B	Fe–27Mn–3Si	71.9	25.6	2.5	
C	Fe–28Mn–2Si	72.3	25.0	2.7	
D	Fe–28Mn–3Si	68.9	26.8	4.3	
E	Fe–30.5Mn–5Si	65.0	30.1	4.9	
F	Fe–32Mn–4Si	64.2	32.2	3.6	
G	Fe–30.5Mn–4.5Si–0.5P	64.5	32.0	3.0	0.5
H	Fe–30.5Mn–4Si–1P	63.6	32.0	3.4	1.0
I	Fe–30.5Mn–3.5Si–1.5P	66.2	30.1	2.4	1.3

Table 1: Chemical composition (mean values) of the alloys investigated

Results and Discussion

For manufacturing of shape memory alloys the appearance of a homogeneous high–temperature phase directly from the liquid is of great importance. As mentioned above, this is possible in shape memory alloys on copper–base or NiTi produced by meltspinning (1).

In the case of the chosen Fe–Mn–Si and Fe–Mn–Si–P specimen an austenitic microstructure with fractions of hcp ϵ–martensite was expected at room–temperature.

Optical micrographs of the as–quenched ribbons are shown in Fig. 1:

Different velocities of the spinning wheel (i.e. cooling rates) are leading to different types of solidification. At low cooling–rates (Fig. 1a – 5 m/s) dendritic growth is observed. A transition from coarser to finer dendritic growth becomes evident in Fig. 1b – 15 m/s. At high spinning velocities a homogeneous phase forms directly from the liquid. Fig. 1c – 50 m/s shows austenite grains at the onset of martensitic transformation obtained by massive crystallization. The formation of a grain structure even at low spinning velocities (Fig. 1d – 5 m/s) can be observed by alloying phosphorous to this ternary shape memory alloy. However, only parts of the phosphorous are dissolved, in spite of rapid quenching. Fig. 1d shows austenite grains with volume fractions of martensite and phosphide precipitates. In addition, the grain boundaries are covered with a phase, which was identified by means of diffractometry (Guinier–camera) as MnP. This indicates that only parts of the phosphorous are in solid solution with iron. In Fig. 2 the phase covering of the grain boundaries is illustrated, too.

The TEM–analysis (Fig. 2) reveals the crystallography of transformation in Fe–Mn. The phase transformation fcc → hcp is caused by changing the stacking sequence ABCABC of the parent phase to ABAB in the product phase.

In the case of the Fe–Mn–Si alloys (Fig. 1a–b) no ϵ–martensite can be revealed within the dendritic structure by light microscopy. Scanning electron microscopy and special etching treatments provided evidence for martensite plates, which passed through the dendrites. The as–quenched ribbons show a distinct one–way effect in a bending and reheating test. The occurence of the reverse transformation is supplemented by the calorimetric measurements of the phase transformation temperatures, listed in table 2. The transformation hysteresis amounts to approximately 100 °C for all Fe–Mn–Si specimens. The martensitic transformation is not complete at temperatures below M_f. M_f has to be defined as the temperature at which no further transformation is observed with additional undercooling. The amount of residual austenite was determined by means of diffractometry to values up to 65% The same is true for the Fe–Mn–Si–P alloys.

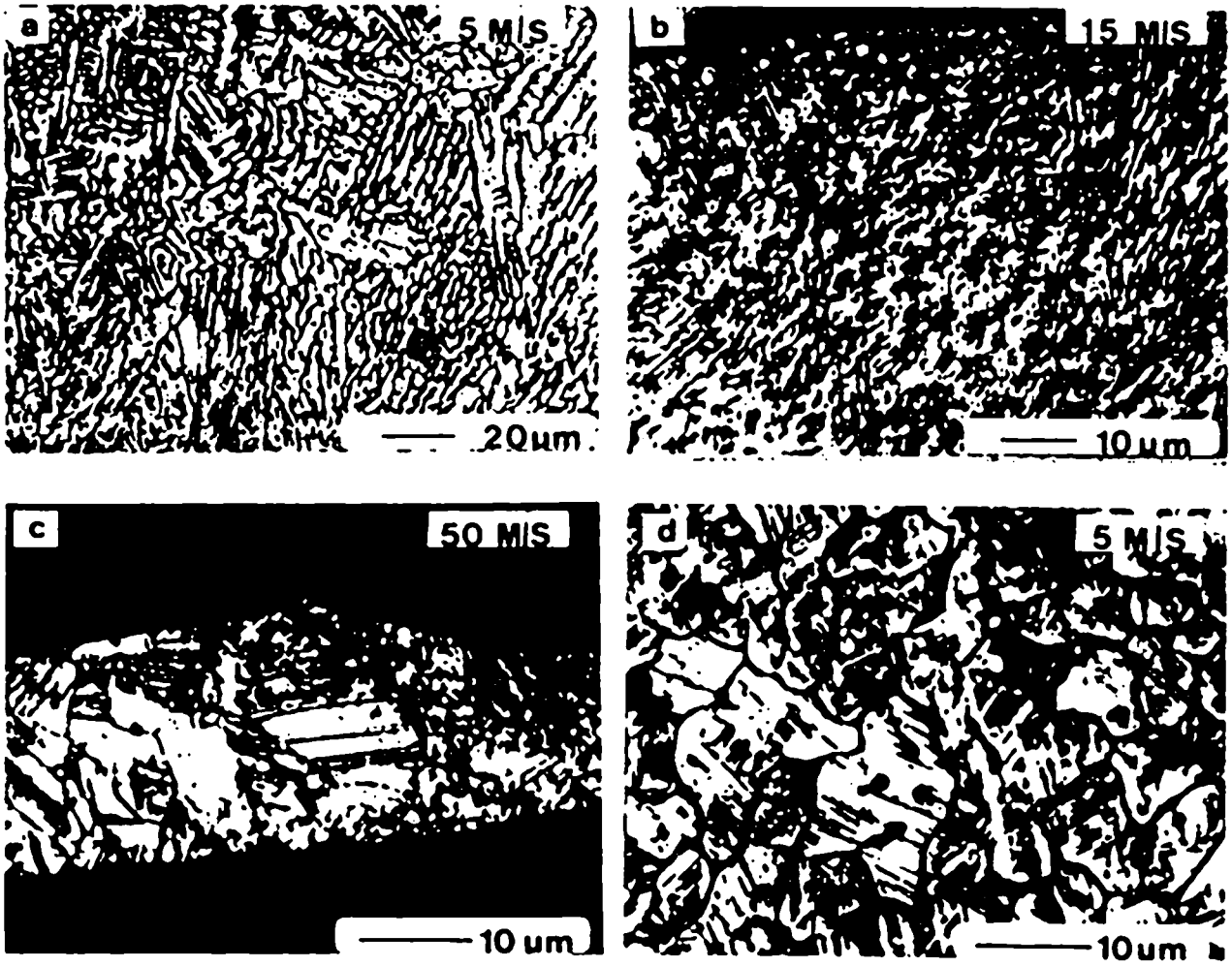

Fig. 1a–d: Light microscopy of cross sections of alloy E (a–c) and G (d). The different wheel circumferential velocities are indicated

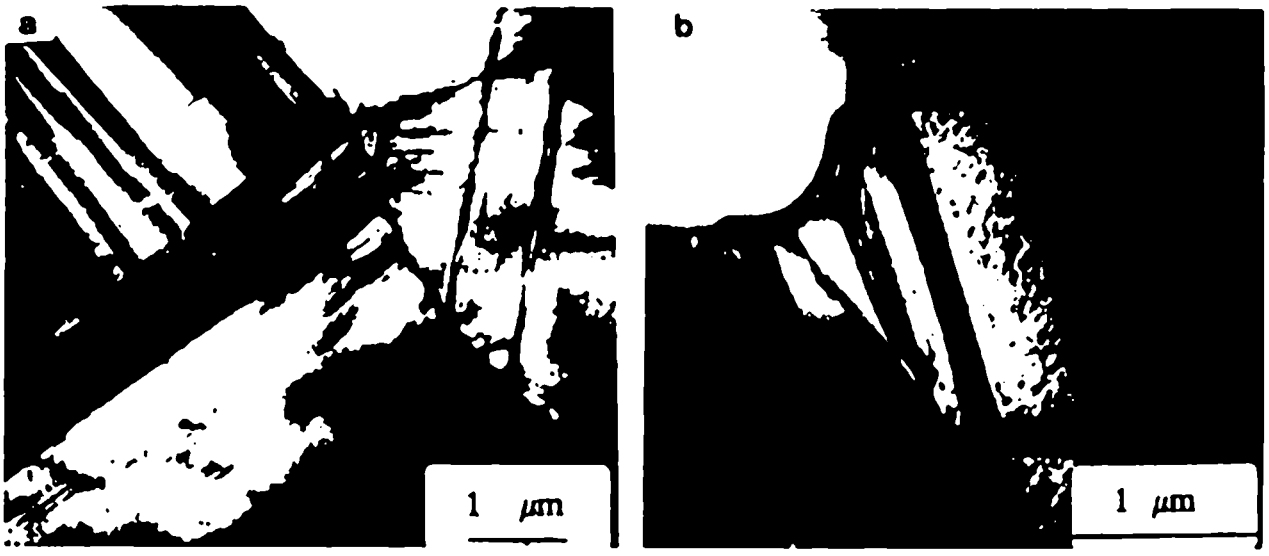

Fig. 2: Transmission electron microscopy of alloy E (a) and G (b)

Alloy	Temperature of as-quenched ribbon [°C]				temperature of heat-treated ribbon [°C]			
	M_s	M_f	A_s	A_f	M_s	M_f	A_s	A_f
A	121	102	197	252	109	85	210	235
B	91	73	186	215	77	53	191	225
C	64	35	199	220	59	15	177	217
D	69	40	168	183	82	53	180	205
E	37	5	155	193	43	1	158	184
F	23	−3	128	158				

Table 2: Typical transformation temperatures of the alloys in the different states as indicated

The phase transformation temperatures of these alloys could not yet be measured by calorimetry. The course of the transformation to the high and low temperature phase seems to be extended in such way that no distinct effect could be measured. This is corroborated by experiments, in which the course of the transformation was investigated under load (Fig. 3). The ribbon is tensile stressed and passes a complete cycle in the temperature range between −100 °C and 300 °C, starting at room-temperature. The temperature ranges M_s–M_f and A_s–A_f are approximately 100 °C in each case , the whole hysteresis M_f–A_f 230 °C. Since the transformation hysteresis gets even smaller under external stress for Fe-Mn-Si alloys (70 °C), the retardation of the transformation caused by the addition of phosphorous becomes evident. The martensitic transformation is obtained by undercooling and external stress. The martensite crystals,which still exist at room-temperature, are re-oriented by an applied stress above the yield stress. Further cooling leads to additional transformation. The re-transformation is delayed. It is getting started only after an essential reduction of the applied load because of a small working-ability.

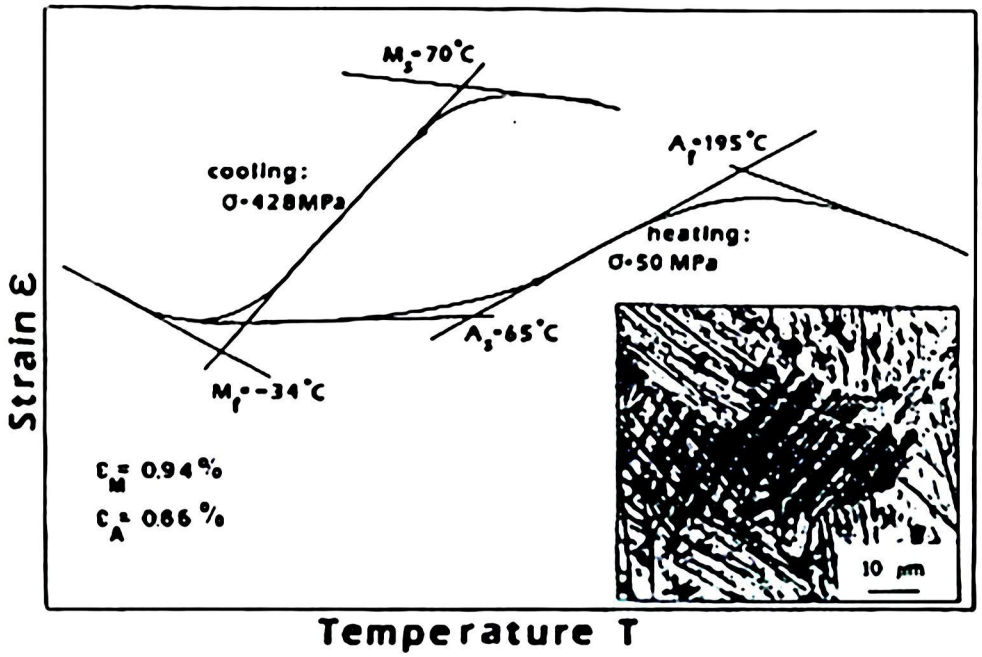

Fig. 3: Transformation temperatures of alloy G (re-austenitized at 1000 °C/1 h) under constant load. The amount of strain in the different states is indicated

Obviously no strenghtening mechanism can be obtained by alloying phosphorous. That can be observed in Fig. 4. Only at high P–contents, above the maximum solubility in γ–iron, an increased hardness can be obtained. However, these specimen show brittleness in tensile tests. Alloys with amounts of phosphorous up to 0.5 wt.% exhibit greater elongations at fracture than the ternary alloys (Fig. 5). The MnP–phase at the grain boundaries in fact impedes the shape memory effect. It favours plastic flow of the material in tensile tests by reducing brittleness due to segregation at the grain boundaries.

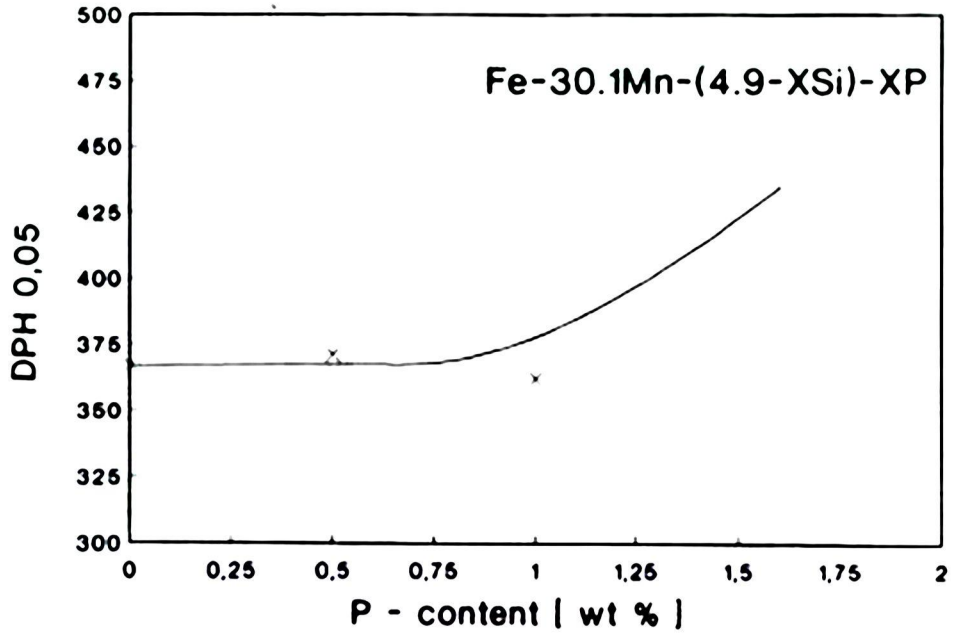

Fig. 4: Course of hardness in dependence of P–content (mean values of 5 measurements)

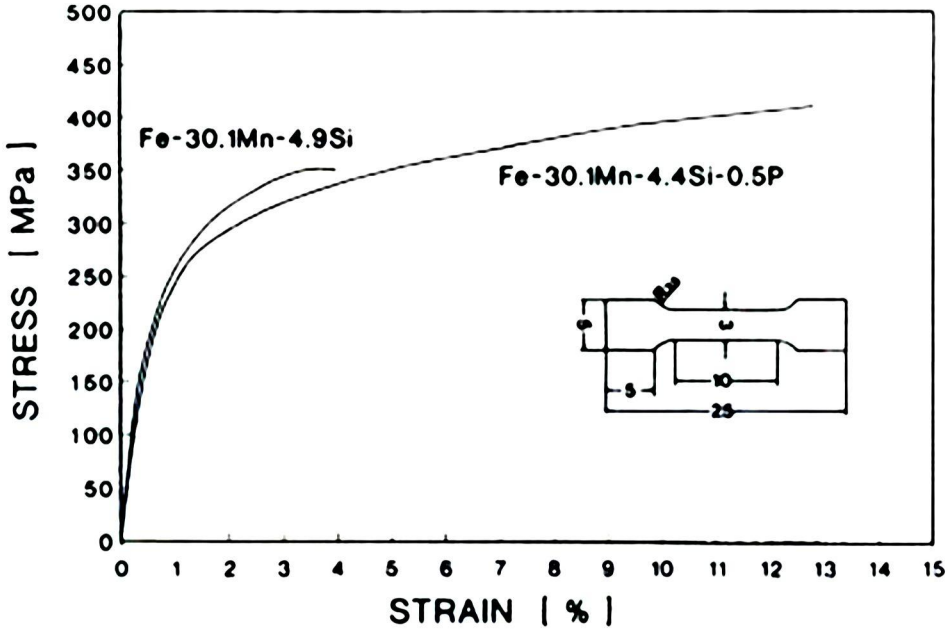

Fig. 5: Comparison of stress–strain curves of alloy E and G (as–quenched state)

The as–quenched Fe–Mn–Si ribbons show a considerable one–way effect. A re–austenitization (1h, 1000 °C) leads to no remarkable change of the effect and the phase transformation temperatures (Table 2). The mechanical properties are not either influenced by the re–heat–treatment. Fig. 6 indicates that there are no major differences between the

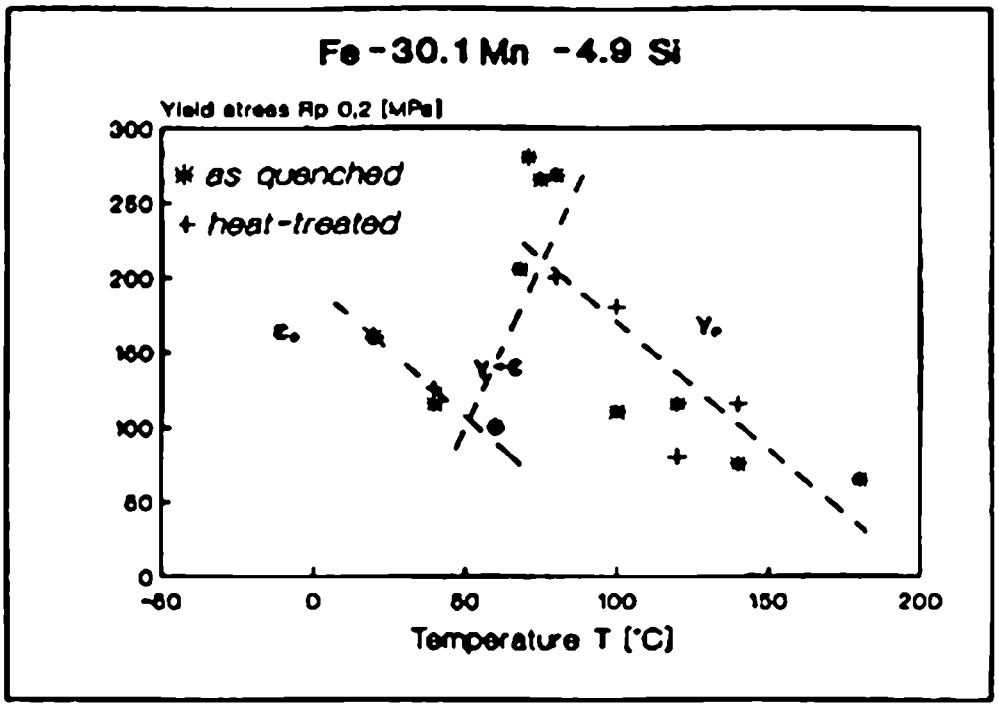

Fig. 6: Results of tensile tests of as-quenched and heat-treated ribbons

as-quenched and heat-treated state. The temperature dependence of the yield stress is shown. At higher temperatures an increase of the yield stress in the austenite state can be observed. Towards lower temperatures the yield stress appears to decrease as a consequence of the stress induced $\gamma \rightarrow \epsilon$-transformation. At temperatures below M_f the yield stress increases again. No additional stress induced transformation occurs and the temperature dependence of the non-transforming phases becomes effective.

Conclusions

Ternary Fe-Mn-Si alloys show a considerable one-way effect after meltspinning, in spite of their dendritic structure. The ribbons can not excert high forces. They nevertheless are suitable as semifinished products for one-way applications.
Alloying of phosphorous does not lead to the expected strenghtening due to lack of solubility. The as-quenched state shows a small one-way effect. Re-austenitization treatment leads to an improvement of the one-way effect in this quaternary alloys (Fig. 3). An exploratory study is under way with alloying elements, which are expected to favour hardening of austenite by short range order (Zn or Ga) to increase the strength of the alloys.

Acknowledgement

The support of the Ministry of Science and Technology (BMFT 03M5006B5) is gratefully acknowledged.

References

(1) S. Eucken, Schmelzspinnen von Legierungen mit Formgedächtnis, VDI-Fortschrittberichte, Reihe 5, Nr. 119, (1987).
(2) A. Sato, Y. Yamaji and T. Mori, Acta metall. 34, No. 2 (1986) 287-294.
(3) Shape Memory Alloy and Method for Producing the Same, 0176272 A1 European Patent Office